**IOP** Publishing Journal Title
Journal **XX** (XXXX) XXXXXX https://doi.org/XXXX/XXXX

# Low-temperature growth of $n^{++}$-GaN by metalorganic chemical vapor deposition to achieve low-resistivity tunnel junctions on blue light emitting diodes

**Pirouz Sohi[1], Mauro Mosca[1,2], Yao Chen[1], Jean-François Carlin[1] and Nicolas Grandjean[1]**

[1] Institute of Physics, Ecole polytechnique fédérale de Lausanne (EPFL), CH-1015 Lausanne, Switzerland

[2] Department of Energy, Information engineering and Mathematical models (DEIM), University of Palermo, IT-90128 Palermo, Italy

E-mail: pirouz.sohi@epfl.ch

Received xxxxxx
Accepted for publication xxxxxx
Published xxxxxx

## Abstract

We report on low-resistivity GaN tunnel junctions (TJ) on blue light-emitting diodes (LEDs). Si-doped $n^{++}$-GaN layers are grown by metalorganic chemical vapor deposition directly on LED epiwafers. Low growth temperature (< 800 °C) was used to hinder Mg-passivation by hydrogen in the $p^{++}$-GaN top surface. This allows achieving low-resistivity TJs without the need for post-growth Mg activation. TJs are further improved by inserting a 5 nm thick $In_{0.15}Ga_{0.85}N$ interlayer (IL) within the GaN TJ thanks to piezoelectric polarization induced band bending. Eventually, the impact of InGaN IL on the internal quantum efficiency of blue LEDs is discussed.

Keywords: GaN tunnel junctions, metalorganic chemical vapor deposition, blue light-emitting diodes

## 1. Introduction

Development of high-efficiency blue and white light-emitting diodes (LEDs) as well as blue laser diodes (LDs) is of utmost importance in the framework of energy-efficient lighting [1, 2]. At present, the III-nitride (III-N) materials system has established itself as the reference on the solid-state lighting market. However, high-power visible LEDs still suffer from issues related to efficiency droop, which pulls down the quantum efficiency of LEDs at high driving current density. To overcome the detrimental impact of droop efficiency on high-power LEDs, Akyol *et al.* [3] proposed an original approach based on cascaded LEDs connected by tunnel junctions (TJs). In addition, TJs could be an alternative solution to indium-tin-oxide (ITO) transparent contacts not only for high-power LEDs, but also for GaN-based ultraviolet LEDs [4], white LEDs [5], microLEDs [6], LDs [7, 8], and vertical cavity surface emitting lasers (VCSELs) [9]. TJs could alleviate the high absorption of the ITO layer at short wavelengths and its relatively high contact resistance [10]. Along this, TJ contacts have proven to be an excellent alternative to metallic contact as demonstrated by Yonkee *et al.,* who reported blue LEDs with external quantum efficiency (EQE) exceeding 70% [11]. TJs also show beneficial effects for green LEDs, where a reduction in droop efficiency has been recently demonstrated [12]. Despite low tunneling probability due to both wide band gap and large effective mass, III-N-based TJs exhibit excellent electrical

 

characteristics likely due to defect assisted tunneling processes. In addition, TJs may benefit from the high polarization field inherent to *c*-plane grown quantum heterostructures, which by inducing a strong band bending makes the tunneling process more favorable. The first InGaN/GaN-based TJs, initially developed by metalorganic chemical vapor deposition (MOCVD), were demonstrated in 2001 by Takeuchi *et al*. [13]. In 2010, Krishnamoorthy *et al.* reported low-resistivity InGaN/GaN-based TJs [14] using molecular beam epitaxy (MBE) instead of MOCVD. MBE allows for low growth temperatures and hydrogen-free environment, hindering therefore passivation of the Mg acceptor, hence leading to significant improvement in the TJ electrical properties. In 2013, the specific differential resistance $\rho_{sd}$ of an InGaN-based TJ grown by plasma-assisted MBE reached the record low value of $1.2 \times 10^{-4}$ Ω cm$^2$ [15]. Recently, Malinverni *et al*. [6] reported on microLEDs featuring GaN-based TJs grown by $NH_3$-MBE without using InGaN interlayers (IL), while still exhibiting excellent electrical properties ($\rho_{sd} = 3.7 \times 10^{-4}$ Ω cm$^2$ at 2.5 kA/cm$^2$). In 2016, the University of California at Santa Barbara proposed a straightforward but dramatically powerful approach consisting in the deposition at low temperature of a $n^{++}$-GaN layer by MBE directly on activated $p^{++}$-GaN top layer surface [16]. This led to high performance devices such as conventional [16] and high-reflectivity LEDs [11], LDs [7], VCSELs [9], and white LEDs [17].

On the other hand, MOCVD is the standard growth technique for manufacturing III-N-based optoelectronic devices because of the high internal quantum efficiency of InGaN/GaN quantum well (QW) active region and large growth rates it offers in comparison to MBE. All-MOCVD grown GaN-based TJs would thus be highly desirable. However, during the growth of the $n^{++}$-GaN layers, hydrogen may passivate the Mg acceptor in the $p^{++}$-layer. Mg passivation starts at temperature as low as 500°C in $NH_3$ atmosphere [18], which corresponds to the temperature of $NH_3$ decomposition [19]. To overcome this parasitic reaction, post-growth annealing is usually performed in order to break Mg-H complexes and hence activate Mg acceptors. Unfortunately, in TJ based LEDs the Mg-doped GaN layer is buried by an *n*-type layer, which hinders the diffusion of hydrogen [20, 21]. Thus, the only way to get rid of hydrogen is through the side walls of an etched mesa structure [22]. In 2016, Takasuka *et al*. [23] reported all-MOCVD grown low-resistivity ($\rho_{sd}$ = 2.3 × $10^{-4}$ Ω cm$^2$ at 3 kA/cm$^2$) TJs by annealing an etched circular mesa structure under oxygen ambient at 725°C for 30 min, the mesas being 35 µm in diameter. Such lateral activation scheme is thus well adapted for VCSELs but might induce severe limitations for large area LEDs. As an illustration, increasing the size of the mesa to 1 mm-side leads to long thermal annealing times and a high thermal budget (800°C, 60 min), which proves detrimental in terms of $\rho_{sd}$ value of the TJ ($2.6 \times 10^{-1}$ Ω cm$^2$ at 10 A/cm$^2$) [24]. Furthermore, a high thermal budget may degrade the InGaN IL in TJs and/or the efficiency of high In content InGaN/GaN QWs in long wavelength LEDs. Therefore, one solution would be to deposit by MOCVD an $n^{++}$-GaN layer on top of the activated $p^{++}$-GaN layer and form thereby the TJ without parasitic Mg passivation during growth, as demonstrated by MBE grown TJs [16].

In this paper, we report on MOCVD growth at low temperature of $n^{++}$-GaN layers with the aim of achieving TJs on blue LEDs. Si-doped GaN layers with electron concentration exceeding $10^{20}$ cm$^{-3}$ are synthesized at 740 °C while keeping a smooth surface morphology. Deposition of such an $n^{++}$-layer on top of an activated blue LED epiwafer allows for the realization of efficient TJs. In addition, we investigate the impact of both InGaN (with different thicknesses and indium contents) and AlInN IL on the electrical characteristics and EQE of TJ based blue LEDs.

## 2. Experimental

Si-doped $n^{++}$-GaN layers were deposited on 2 µm thick non-intentionally doped (UID) GaN templates grown on *c*-plane sapphire substrates (figure 1(a)) at a growth rate of ~ 100 nm/h. These samples were grown in an Aixtron 200/4 RF-S reactor in a 540 to 770 °C temperature range, with various silane flows, and at a pressure of 200 mbar. For the $n^{++}$-GaN layers, the precursors and carrier gases were triethylgallium (TEGa), $NH_3$, silane (diluted to 100 ppm in $H_2$) and $N_2$, respectively. Carrier density, mobility and resistivity of these layers were obtained by room-temperature Hall effect measurements. The $n^{++}$-GaN layer thickness was comprised between 50 and 70 nm. The structure of the samples used for this study is shown in figure 1(a).

The TJs were formed by depositing $n^{++}$-type layers directly on activated 455 nm LED epiwafers supplied by PAM-XIAMEN. Both LED and TJ structure are displayed in figure 1(b). Five different kind of samples were prepared, differing by the type of IL, as reported in Table 1. The InGaN IL was grown at 700 °C using trimethylindium (TMIn) and TEGa while for the AlInN IL, lattice-matched to GaN with an indium content of 18 %, the growth was performed at 775 °C using TMIn and trimethylaluminum as precursors. All the ILs were heavily doped ($n$ = 1 - 2 × $10^{20}$ cm$^{-3}$). LEDs (100 × 100 µm$^2$) were fabricated using standard photolithographic process and inductively coupled plasma reactive ion etching. Ti/Al/Ti/Au metal stacked layers were used for both top and bottom contacts. A standard *p*-contact LED was fabricated from a bare LED epiwafer (without TJ) for the sake of comparison. For this latter sample, *p*-type and *n*-type contacts were made with Pd/Au and Ti/Al/Ti/Au stacks, respectively.

## 3. Results and discussion

Figure 2 shows the effect of the growth temperature on the electrical properties of the Si-doped GaN layers. The silane flow rate was fixed at 6 sccm, while for all the experiments the $NH_3$ flow was 2000 sccm. Both carrier density and mobility decrease with temperature, and consequently, the resistivity increases (figures 2(a)-(c)). This is likely due to an enhancement of carbon incorporation when reducing the growth temperature [25], which results in Si compensation. The surface morphology investigated by atomic force microscopy (AFM) displays granular-like features below 700 °C due to low surface kinetics (figure 2(d) and 2(e)). The grain sizes increase with temperature leading to coalescence and eventually to a continuous two-dimensional surface morphology above 770 °C (figure 2(f)). This temperature-dependent study demonstrates that heavily Si-doped ($n \geq 10^{20}$ $cm^{-3}$) thin GaN layers with decent surface morphology can be achieved below 800 °C. Then, the electrical properties were further optimized by varying the silane flow rate at a temperature of 740 °C. Heavily *n*-doped ($n \geq 10^{20}$ $cm^{-3}$) layers are obtained for silane flows larger than 4 sccm, however with a slight degradation of the overall electrical properties above 10 sccm (figures 3(a)-(c)). This results in a minimum resistivity of 7- 8 × $10^{-4}$ Ω cm for a silane flow ranging between 2 and 8 sccm (figure 3(a)). On the other hand, the surface morphology roughens dramatically with increasing silane flow: at low flow rates (0.6 sccm), the surface exhibits pits (figure 3(d)), whose density increases for larger flow (figure 3(e)), leading eventually to quite rough surface morphology (figure 3(f)).

The actual TJ structure was designed according to the dependence of the $n^{++}$-GaN layer properties on silane flow and growth temperature, and keeping in mind potential parasitic passivation of Mg in the $p^{++}$-GaN top layer surface. Thus, a thin (5 nm) $n^{++}$-GaN layer is deposited at 700 °C directly on the activated LED epiwafer (sample A). Then, a 150 nm $n^{+}$-GaN spreading layer ($n$ = 1 - 2 × $10^{19}$ $cm^{-3}$) is grown at slightly higher temperature (740 °C) to keep a smooth surface morphology. Finally, a 10 nm $n^{++}$-GaN cap layer is grown at 740 °C ($n$ = 1 - 2 × $10^{20}$ $cm^{-3}$). The silane flow rate is fixed at 6.7 sccm. Notice that for samples (B - D), the InGaN IL is grown at 700 °C while in the case of AlInN IL (E), the growth temperature is 775 °C in order to incorporate 18% indium as required to ensure lattice-matching to GaN.

Figure 4(a) shows the *J-V* characteristics of LEDs with different types of TJs, together with the characteristics of the *p*-contact LED. The inset shows the same characteristics at lower current density. For sake of comparison, we look at the forward voltage at 1 A/$cm^2$, for which the contribution of the contact resistance is negligible (figure 4(b)). For the *p*-contact LED (without TJ), the forward voltage is as low as 2.58 V, in agreement with a nearly ideal InGaN/GaN QW *p-n* junction [26]. The forward voltage increases to 2.85 V for pure GaN TJ (sample A) but reduces when introducing a 5 nm thick InGaN IL (samples B and C): 2.80 V and 2.67 V for 10 % and 15 % In content, respectively. The better electrical characteristics of InGaN based TJs is in line with previous reports [14, 23]. This improvement can be definitively ascribed to polarization-assisted band bending rather than indium-related point defect assisted tunneling. Indeed, a reduction of the $In_{0.15}Ga_{0.85}N$ IL thickness from 5 nm to 1 nm (sample D) leads to an increase of the forward voltage. More striking, we inserted a 5 nm thick $Al_{0.82}In_{0.18}N$ IL and observed a strong degradation of the TJ, i.e. a forward voltage at 1 A/$cm^2$ of 3.60 V. This is consistent with a lower tunneling probability due to the large band gap of $Al_{0.82}In_{0.18}N$ (~4.5 eV).

The specific differential resistances ($\rho_{sd}$) of the whole devices measured at 1.5 kA/$cm^2$ are reported in figure 4(c). The differential resistance of the TJ itself should be lower than these values, which are of the same order of magnitude than those reported for MOCVD- and MBE-grown TJs [6, 15, 16, 23, 24]. All the LEDs with InGaN IL (samples B, C and D) have a similar differential resistance, the one without IL (sample A) has a slightly higher resistance, and the LED with the AlInN IL (sample E) has an even higher resistance. Sample D exhibits the lowest value (8.6 × $10^{-4}$ Ω $cm^2$ at 1.5 kA/$cm^2$).

In previous studies on MOCVD-grown TJs [22-24], post-growth Mg activation was achieved through mesa side walls. Such an approach, although proven to be suitable, may encounter some limitations, especially for large mesa sizes. For instance, the forward voltage at 1 A/$cm^2$ measured on 1 × 1 $mm^2$ mesa structures after 60 minutes thermal annealing at 800 °C is around 5 V for GaN TJ-based LEDs [24]. Instead, the deposition at low temperature of $n^{++}$-GaN (or InGaN) on $p^{++}$-GaN layers eliminates the need for lateral Mg activation. TJ-based LEDs can actually be formed this way in a single run: epitaxial growth of LED structure first, followed by *in situ* Mg activation of the $p^{++}$-GaN layer and finally growth at low temperature of the $n^{++}$-GaN layer to form the TJ.

III-N-based TJs entirely grown by MOCVD have therefore the potential to enable novel devices like multi-junction LEDs or to increase the EQE of blue-violet LEDs thanks to lower optical losses as compared to standard ITO contacts. Then arises the question of the potential absorption of the InGaN IL, especially for the high In content alloy. We thus measured the EQE of the TJ-LEDs (figure 5). Notice that in our experimental setup, the EQE is measured from the backside of the planar device and therefore is significantly underestimated. However, we can still conduct a side-by-side comparison and probe the optical losses induced by the different ILs since the light cone directed toward the top surface is partly reflected toward the sapphire substrate. The maximum EQE ($EQE_{max}$) was observed for current densities in the range of 2.5 to 3.8 A/$cm^2$, which is consistent with the

results found by David *et al.* [26] for high-efficiency blue LEDs.

It is worth pointing out that light extraction was not optimized for the present TJ-based LEDs: the 170 nm thick multilayer structure grown on top of the LED structure makes the optical field maximum and the QWs no longer perfectly matching, which explains the lower EQE of TJ-LEDs compared to that of the *p*-contact LED. Moreover, the LED without a TJ uses a different metal (Pd) as a top contact which has a different reflectivity than Ti/Al, used for contacting TJs.

The highest value of the EQE peak for TJ-LEDs is reached for sample E (AlInN IL), followed by sample A (no IL). This is illustrated in the inset of figure 5, which displays $EQE_{max}$ for the different LED samples. The slightly higher EQE for AlInN IL may indicate that $n^{++}$-GaN already introduces losses due to band tailing. On the other hand, sample C exhibits the lowest $EQE_{max}$ due to the strong absorption occurring in the 5 nm thick $In_{0.15}Ga_{0.85}N$ IL. Between these two extreme cases, the EQE peak value increases with decreasing indium content in the InGaN IL (sample B). Therefore, high In content InGaN ILs facilitate tunneling processes but at the expense of optical losses. Reducing the thickness of the $In_{0.15}Ga_{0.85}N$ IL to 1 nm (sample D) leads to an increase in the EQE but, as already discussed, the electrical properties degrade due to insufficient band bending. Eventually, a reduction in the IL thickness, keeping the In content high, gives nearly the same results as a reduction in the In content while keeping the IL thickness unchanged (cf. samples B and D). From these findings, one does conclude that efficient TJs must feature a high In content InGaN IL, which has to be thick enough and be located at the antinode of the optical field to limit the absorption losses.

## 4. Conclusions

We have shown that $n^{++}$-GaN ($n \geq 10^{20}$ cm$^{-3}$) layers can be grown by MOCVD at low temperatures, *i.e.* in the 700 to 750°C range. This allows hindering the parasitic hydrogen passivation of activated Mg-doped layers during III-N $n^{++}$-layers overgrowth. This way, TJs have been achieved on top of blue LED epiwafers, which were *ex situ* activated beforehand. The effects of an IL (InGaN or AlInN) inserted in the GaN TJ has been investigated. A total differential resistance as low as $8.6 \times 10^{-4}$ Ω cm$^2$, and operating voltages of 2.67 V at 1 A/cm$^2$ and 3.28 V at 20 A/cm$^2$, have been obtained using a 5 nm thick $In_{0.15}Ga_{0.85}N$ IL. These results pave the way for large-scale production of nitride-based TJ LEDs using MOCVD.

## Acknowledgements

The authors wish to thank Dr. Raphaël Butté for critical reading of the manuscript.

## References

[1] DenBaars S P, Feezell D, Kelchner K, Pimputkar S, Pan C-C, Yen C-C, Tanaka S, Zhao Y, Pfaff N, Farrell R, Iza M, Keller S, Mishra U, Speck J S and Nakamura S 2013 Development of gallium-nitride-based light-emitting diodes (LEDs) and laser diodes for energy-efficient lighting and displays *Acta Materialia* **61** 945–51

[2] Denault K A, Cantore M, Nakamura S, DenBaars S P and Seshadri R 2013 Efficient and stable laser-driven white lighting *AIP Advances* **3** 072107

[3] Akyol F, Krishnamoorthy S and Rajan S 2013 Tunneling-based carrier regeneration in cascaded GaN light emitting diodes to overcome efficiency droop *Applied Physics Letters* **103** 081107

[4] Sadaf S M, Zhao S, Wu Y, Ra Y-H, Liu X, Vanka S and Mi Z 2017 An AlGaN Core–Shell Tunnel Junction Nanowire Light-Emitting Diode Operating in the Ultraviolet-C Band *Nano Letters* **17** 1212–8

[5] Lam K-T, Lin W-H, Shei S-C, Lin N-M, Chen W-S and Chang S-J 2016 White-Light Emission From GaN-Based TJ LEDs Coated With Red Phosphor *IEEE Electron Device Letters* **37** 1150–3

[6] Malinverni M, Martin D and Grandjean N 2015 InGaN based micro light emitting diodes featuring a buried GaN tunnel junction *Applied Physics Letters* **107** 051107

[7] Yonkee B P, Young E C, Lee C, Leonard J T, DenBaars S P, Speck J S and Nakamura S 2016 Demonstration of a III-nitride edge-emitting laser diode utilizing a GaN tunnel junction contact *Optics Express* **24** 7816

[8] Malinverni M, Tardy C, Rossetti M, Castiglia A, Duelk M, Vélez C, Martin D and Grandjean N 2016 InGaN laser diode with metal-free laser ridge using n $^+$ -GaN contact layers *Applied Physics Express* **9** 061004

[9] Leonard J T, Young E C, Yonkee B P, Cohen D A, Margalith T, DenBaars S P, Speck J S and Nakamura S 2015 Demonstration of a III-nitride vertical-cavity surface-emitting laser with a III-nitride tunnel junction intracavity contact *Applied Physics Letters* **107** 091105

[10] Takehara K, Takeda K, Nagata K, Sakurai H, Ito S, Iwaya M, Takeuchi T, Kamiyama S, Akasaki I and Amano H 2011 Transparent electrode for UV light-emitting-diodes *Physica status solidi (c)* **8** 2375–7

[11] Yonkee B P, Young E C, DenBaars S P, Nakamura S and Speck J S 2016 Silver free III-nitride flip chip light-emitting-diode with wall plug efficiency over 70% utilizing a GaN tunnel junction *Applied Physics Letters* **109** 191104

[12] Alhassan A I, Young E C, Alyamani A Y, Albadri A, Nakamura S, DenBaars S P and Speck J S 2018 Reduced-droop green III–nitride light-emitting diodes utilizing GaN tunnel junction *Appl. Phys. Express* **11** 042101

[13] Takeuchi T, Hasnain G, Corzine S, Hueschen M, Schneider, Jr. R P, Kocot C, Blomqvist M, Chang Y, Lefforge D, Krames M R, Cook L W and Stockman S A 2001 GaN-Based Light Emitting Diodes with Tunnel Junctions *Japanese Journal of Applied Physics* **40** L861–3

[14] Krishnamoorthy S, Nath D N, Akyol F, Park P S, Esposto M and Rajan S 2010 Polarization-engineered GaN/InGaN/GaN tunnel diodes *Applied Physics Letters* **97** 203502

[15] Krishnamoorthy S, Akyol F, Park P S and Rajan S 2013 Low resistance GaN/InGaN/GaN tunnel junctions *Applied Physics Letters* **102** 113503

[16] Young E C, Yonkee B P, Wu F, Oh S H, DenBaars S P, Nakamura S and Speck J S 2016 Hybrid tunnel junction contacts to III–nitride light-emitting diodes *Applied Physics Express* **9** 022102

[17] Kowsz S J, Young E C, Yonkee B P, Pynn C D, Farrell R M, Speck J S, DenBaars S P and Nakamura S 2017 Using tunnel junctions to grow monolithically integrated optically pumped semipolar III-nitride yellow quantum wells on top of electrically injected blue quantum wells *Optics Express* **25** 3841

[18] Nakamura S, Iwasa N, Senoh M and Mukai T 1992 Hole Compensation Mechanism of P-Type GaN Films *Jpn. J. Appl. Phys.* **31** 1258

[19] Mesrine M, Grandjean N and Massies J 1998 Efficiency of NH3 as nitrogen source for GaN molecular beam epitaxy *Applied Physics Letters* **72** 350–2

[20] Neugebauer J and Van de Walle C G 1996 Role of hydrogen in doping of GaN *Applied Physics Letters* **68** 1829–31

[21] Pankove J I, Magee C W and Wance R O 1985 Hole-mediated chemisorption of atomic hydrogen in silicon *Applied Physics Letters* **47** 748

[22] Kuwano Y, Kaga M, Morita T, Yamashita K, Yagi K, Iwaya M, Takeuchi T, Kamiyama S and Akasaki I 2013 Lateral Hydrogen Diffusion at p-GaN Layers in Nitride-Based Light Emitting Diodes with Tunnel Junctions *Japanese Journal of Applied Physics* **52** 08JK12

[23] Takasuka D, Akatsuka Y, Ino M, Koide N, Takeuchi T, Iwaya M, Kamiyama S and Akasaki I 2016 GaInN-based tunnel junctions with graded layers *Applied Physics Express* **9** 081005

[24] Neugebauer S, Hoffmann M P, Witte H, Bläsing J, Dadgar A, Strittmatter A, Niermann T, Narodovitch M and Lehmann M 2017 All metalorganic chemical vapor phase epitaxy of p/n-GaN tunnel junction for blue light emitting diode applications *Applied Physics Letters* **110** 102104

[25] Cruz S C, Keller S, Mates T E, Mishra U K and DenBaars S P 2009 Crystallographic orientation dependence of dopant and impurity incorporation in GaN films grown by metalorganic chemical vapor deposition *Journal of Crystal Growth* **311** 3817–23

[26] David A, Hurni C A, Young N G and Craven M D 2016 Electrical properties of III-Nitride LEDs: Recombination-based injection model and theoretical limits to electrical efficiency and electroluminescent cooling *Applied Physics Letters* **109** 083501

## Table and figure captions:

**Table 1.** Thickness, composition and growth temperature of the interlayers.

**Figure 1.** (a) Sample structure used for the study of the low temperature highly Si-doped GaN and (b) of the tunnel junctions grown on commercial LED wafers.

**Figure 2.** Room temperature (a) resistivity, (b) carrier density, and (c) mobility, as a function of growth temperature for heavily Si-doped GaN layers. The silane flow rate is 6 sccm for the whole sample series. 1 x 1 $\mu m^2$ AFM scans of samples grown at (d) 540°C, (e) 650°C, and (f) 770°C. The root-mean square roughness values are 5 nm, 11 nm, and 6 nm, respectively.

**Figure 3.** Room temperature (a) resistivity, (b) carrier density, and (c) mobility, as a function of silane flow rate for heavily Si-doped GaN layers. The growth temperature is 740°C. 5 × 5 $\mu m^2$ AFM images of samples grown with a silane flow rate of (d) 0.6 sccm, (e) 2 sccm, and (f) 4 sccm.

**Figure 4.** (a) *J-V* characteristics of 100 × 100 $\mu m^2$ LEDs fabricated in samples A-E, together with the *p*-contact LED sample. The inset shows the same characteristics at lower current density (≤ 1 $A/cm^2$). (b) LED operating voltage at 1 $A/cm^2$ and (c) specific differential resistance of the whole TJ LED devices measured at 1.5 $kA/cm^2$ for the different samples. The horizontal axes indicate the sample numbering (see Table I).

**Figure 5.** EQE vs. *J* curves of 100 × 100 $\mu m^2$ LEDs fabricated in samples A-E, together with the *p*-contact LED sample. The inset shows the values of the EQE peak ($EQE_{max}$) for the different samples. The horizontal axis indicates the sample numbering.

| Sample | Interlayer (IL) |
|---|---|
| **A** | 5 nm $n^{++}$ GaN (700 °C) |
| **B** | 5 nm $n^{++}$ $In_{0.10}Ga_{0.90}N$ (700 °C) |
| **C** | 5 nm $n^{++}$ $In_{0.15}Ga_{0.85}N$ (700 °C) |
| **D** | 1 nm $n^{++}$ $In_{0.15}Ga_{0.85}N$ (700 °C) |
| **E** | 3 nm $n^{++}$ $Al_{0.82}In_{0.18}N$ (775 °C) |

*Table 1*

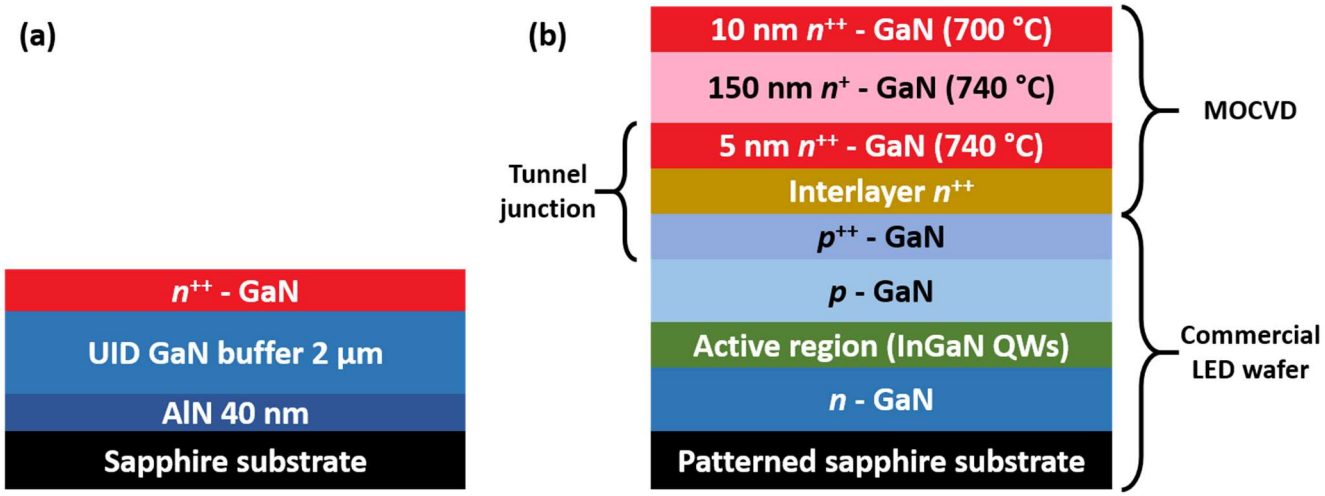


*Figure 1*

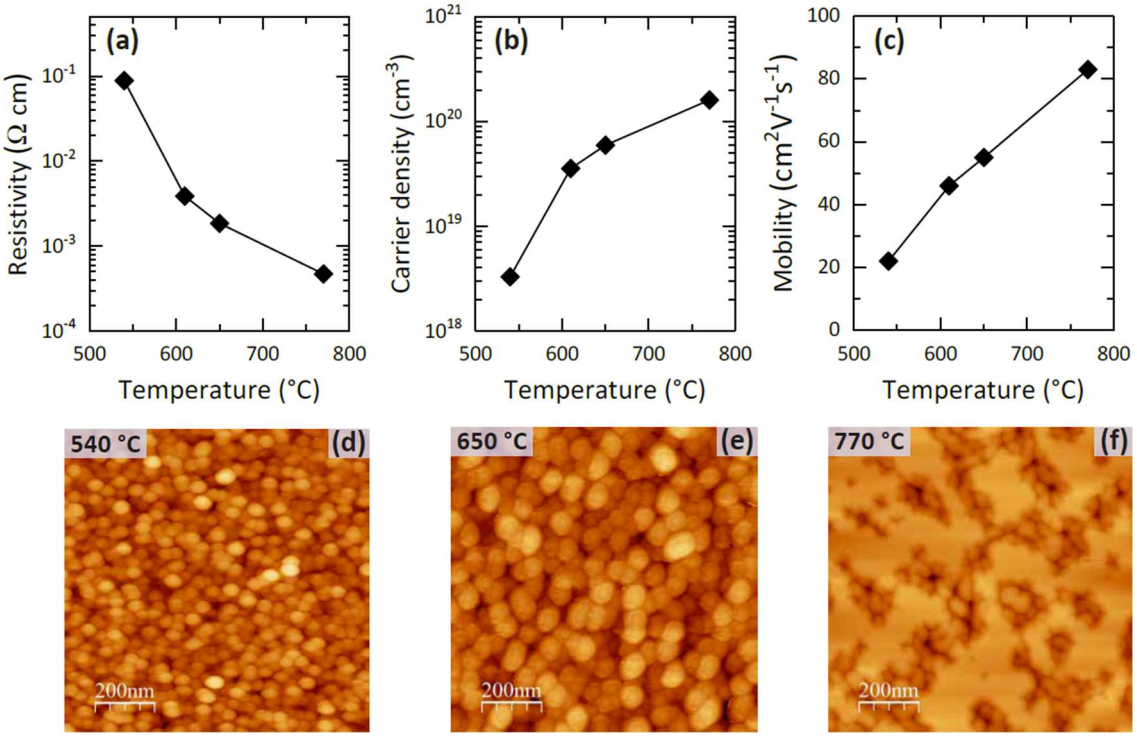


*Figure 2*

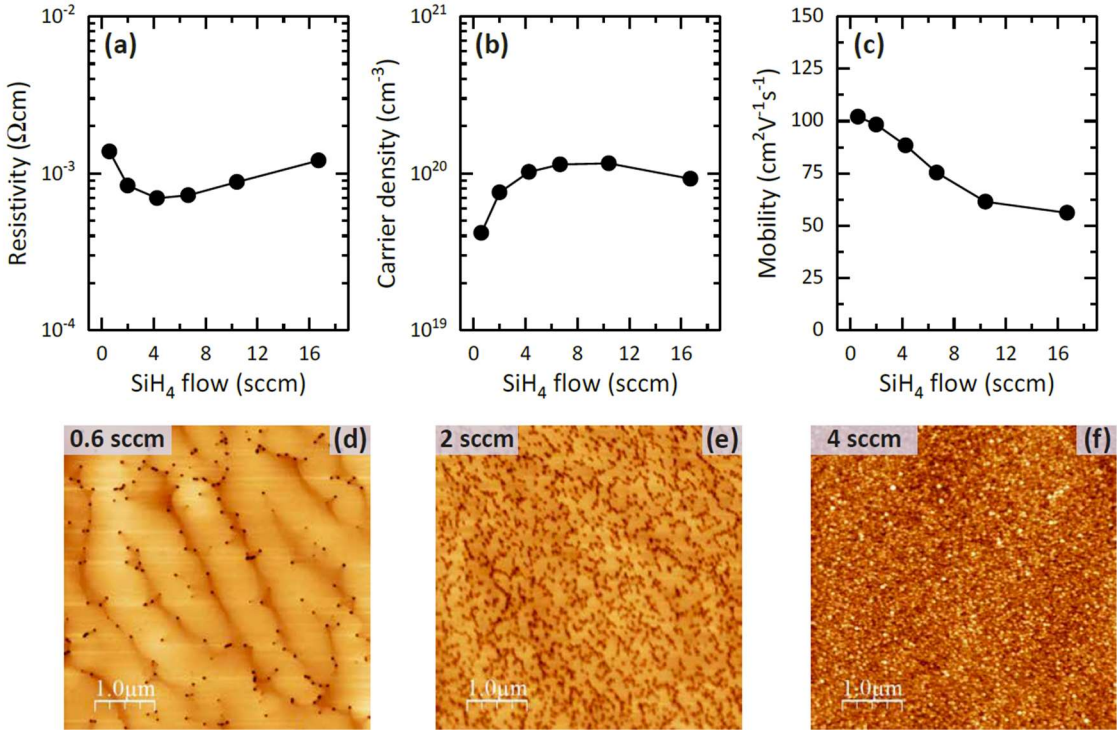


*Figure 3*

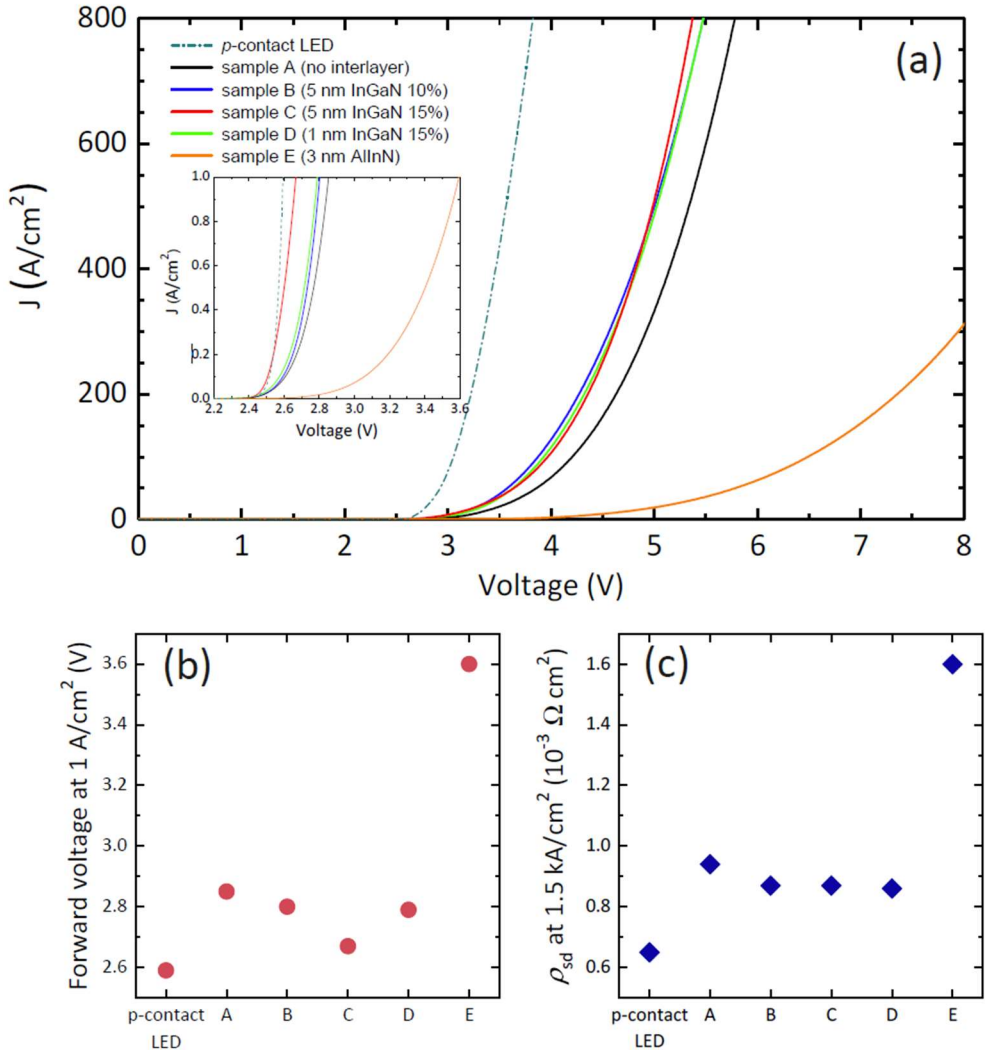
(a)
p-contact LED
sample A (no interlayer)
sample B (5 nm InGaN 10%)
sample C (5 nm InGaN 15%)
sample D (1 nm InGaN 15%)
sample E (3 nm AlInN)
J (A/cm$^2$)
Voltage (V)
(b)
Forward voltage at 1 A/cm$^2$ (V)
(c)
$\rho_{sd}$ at 1.5 kA/cm$^2$ ($10^{-3}$ Ω cm$^2$)
p-contact LED
A
B
C
D
E

*Figure 4*

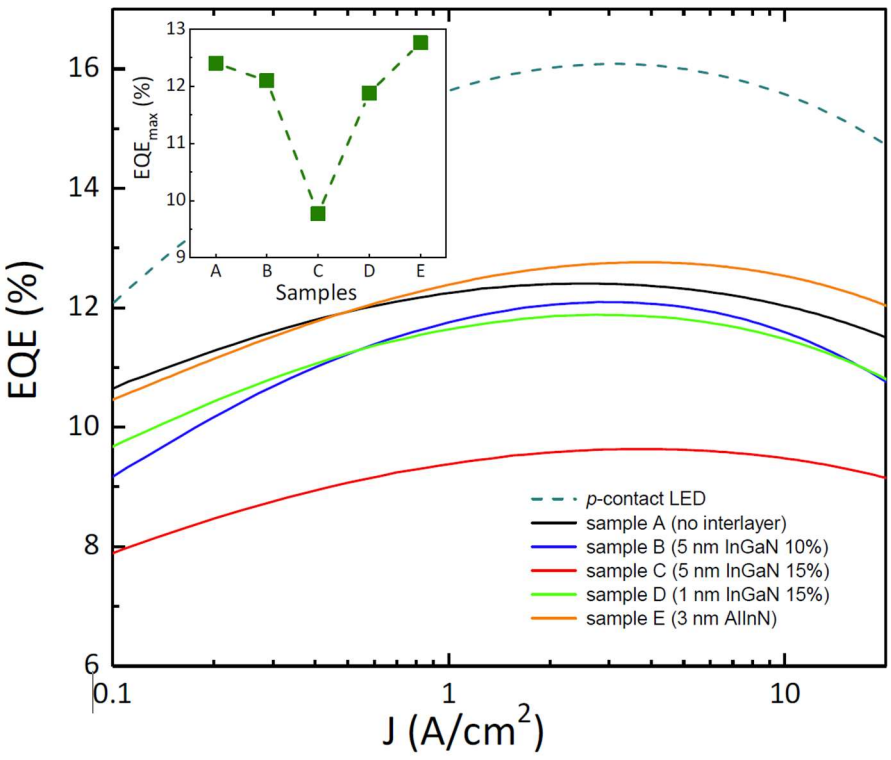
EQE (%)
J (A/cm$^2$)
0.1
1
10
6
8
10
12
14
16
EQE$_{max}$ (%)
9
10
11
12
13
A
B
C
D
E
Samples
*p*-contact LED
sample A (no interlayer)
sample B (5 nm InGaN 10%)
sample C (5 nm InGaN 15%)
sample D (1 nm InGaN 15%)
sample E (3 nm AlInN)

*Figure 5*